Supporting Information

Fully-Biobased Highly Transparent Nanopaper with UV-Blocking Functionality

Douglas R. Hayden[a]‡, Srivatssan Mohan[a]‡, Arnout Imhof [a*], Krassimir P. Velikov[a,b,c]*

[a] Soft Condensed Matter, Debye Institute for Nanomaterials Science, Utrecht University, Princetonplein 1, 3584 CC, Utrecht, the Netherlands.

[b] Unilever R&D Vlaardingen, Olivier van Noortlaan 120, 3133 AT Vlaardingen, the Netherlands

[c] Institute of Physics, University of Amsterdam, Science Park 904, 1098 XH Amsterdam, the Netherlands

‡ These authors contributed equally.

* E-mail: d.r.hayden@uu.nl, a.imhof@uu.nl

EXPERIMENTAL SECTION

Materials

Bacterial cellulose (BC) nanofibrils in the form of pellicles of the strain *Acetobacter* were sourced from a commercial Nata de coco product (Cozzo food industries, Malaysia). Citrus fibers (Herbacel-AQ Plus, type N, ~75% cellulose containing water insoluble fraction) were obtained from Herbafood. Ethyl cellulose (100 cP, lot number MKBT0521V), octinoxate (98%), avobenzone (≥99%), oxybenzone (98%), retinol (≥95%), p-coumaric acid (98%), quercetin (≥95%), and DURAPORE membrane filters (25 mm, pore size 0.65 μm) were obtained from Sigma Aldrich. Ethanol was purchased from Interchema. Deionized water from a Millipore system was used in all experiments.

Preparation of Oxidized Nanofibrils from Bacterial and Citrus Sources

Citrus nanofibril dispersion was prepared by mixing a weighed amount of citrus fibre powder with water, first using a shear mixer (Silverson, L5M-A) for 10 mins at 3000 RPM and then passing it once through a Z-chamber (87 μm channel diameter) in a Microfluidizer™ (Microfluidics Corp, M-110S) operated at a maximum pressure of 1200 bar. Bacterial cellulose pellicles were immersed in a 0.1 M NaOH solution followed by thoroughly washing with water and then breaking it down using a hand blender (Braun 4185545). The resulting BC slurry was then subjected to 8 washing cycles involving vacuum filtration and re-dispersion in water, in order to remove soluble impurities. A macroscopically homogeneous dispersion was obtained after passing the suspension once through the Microfluidizer™ operated at a maximum pressure of 1200 bar. The weight fraction of the nanofibrils in the dispersion was determined gravimetrically, as the average of three samples from which water was evaporated at 45^{o}C under a pressure of 40 mbar in a vacuum oven (Memmert Celcius). A combination of TEMPO-

mediated oxidation reaction and high energy mechanical deagglomeration was applied to disintegrate cellulose nanofibrils from both the sources, described as follows. The oxidation reactions on 0.2 wt% dispersions were done in TEMPO/$NaClO_2$/NaClO system at neutral conditions for 48 hours at 60^{o}C.[1] After the reaction, the oxidized nanofibrils were purified by repeated centrifugation at 10000 g (Hettich Rotina 380R) for 30 mins, decantation and re-dispersion steps, 6 times. In order to individualize the nanofibrils, the purified dispersions were passed through the Microfluidizer™ 5 times, operated at a maximum pressure of 1200 bar. The concentration of the final dispersion was re-measured gravimetrically by the aforementioned procedure.

Preparation of Non-Functionalized Nanopaper Films

Bacterial or citrus cellulose nanofibril dispersion (1 mL at concentration 5 g L^{-1}/0.5 wt%) was vacuum filtrated onto a 22 mm hydrophilic polyvinylidene fluoride membrane filter (pore size 0.65 μm, DURAPORE) cut to fit an 18 mm Buchner funnel for 10 mins until a gel-like cake formed. The filter with the gel-like cake was then removed from the funnel, placed in a petri dish, and put in an oven at 50^{o}C for 10 mins. The nanopaper film was then peeled from the filter with tweezers and pressed for 1 minute with 10 tons of pressure using a hydraulic press (Specac) at room temperature.

Preparation of UV-Absorbing Ethyl Cellulose NPs (Sunscreen-NPs and Biobased-NPs)

Ethyl cellulose NPs with encapsulated UV absorbing molecules were prepared via an antisolvent precipitation technique.[2] Briefly, ethyl cellulose (0.275 g) was dissolved in ethanol (50 mL) along with i) oxybenzone (0.008 g), avobenzone (0.008 g), and octinoxate (0.008 g) for the sunscreen-NPs, or ii) quercetin (0.019 g), p-coumaric acid (0.008 g), and retinol (0.014 g) for the biobased-NPs, before being poured into water (150 mL, pH 5-6) under fast magnetic stirring

resulting in the spontaneous formation of NPs. The dispersions were then evaporated to 50 mL and filtered through filter paper to remove any large aggregates. These dispersions were then concentrated to 10 g L^{-1} (by rotary evaporation, gravimetric determination of concentration and adjustments using water) for the preparation of the UV-blocking nanopaper films.

Preparation of UV-Absorbing Nanopaper Films

Aqueous cellulose nanofibril dispersion (1 mL at concentration 5 g L^{-1}/0.5 wt%) from the citrus source was first mixed with a quantity (0.65 mL of concentration 10 g L^{-1} in Figure 2) of either of the aqueous NP dispersions in a small glass pot. This resultant dispersion was then vacuum filtrated, dried, and pressed as described above.

Characterization

Nanopaper films were characterized with SEM imaging (FEI XL30FEG) in which samples were sputter coated with platinum, direct transmission measurements using a HP 8452a spectrophotometer, total transmission measurements using a home-built set-up with a spectrophotometer (HR4000, Ocean Optics) equipped with a 15 cm diameter integrating sphere (barium sulfate coated, Labsphere) and a Tungsten Halogen light source (HL-2000-FHSA-LL, Ocean Optics), and photographs which were taken with a Nikon D70 camera. NPs were characterized with SEM imaging as described above and also DLS (Malvern Zetasizer Nano ZS) in which particle size distributions were obtained using a CONTIN fitting. Nanofibrils were characterized with SEM imaging as described above and also TEM imaging (Philips TECNAI20) in which the imaged nanofibrils were negatively stained using uranyl acetate and dried on a BUTVAR-coated TEM grid. AFM measurements were used to characterize the surface roughness. Measurements were performed with a JPK Nanowizard II Atomic Force Microscope at room temperature in non-contact mode with a silicon cantilever (BRUKER

model: OTESPA-R3) and the roughness of the films was determined from the height images over a 25 μm^2 area and are presented as root-mean-square (rms) values. Thermogravimetric analysis (TGA) was performed with a TGA Q50 V6.7 Build 203, using approximately 2-3 mg of the respective samples, under an air atmosphere with a ramp of 15.00 °C/min to 800.00 °C. Printing of text onto the film was performed by sticking the nanopaper onto a sheet of A4 paper with tape and subsequent printing using a Xerox WorkCentre 7855.

SUPPLEMENTARY RESULTS

1) Ethyl Cellulose Nanoparticles (NPs) Characterization

Both the sunscreen-NPs and biobased-NPs were characterized with Dynamic Light Scattering (DLS), Scanning Electron Microscopy (SEM) imaging, and absorbance measurements. The DLS measurements show an average particle diameter of 70 nm for the sunscreen NPs and 90 nm for the biobased-NPs (Figure S1).

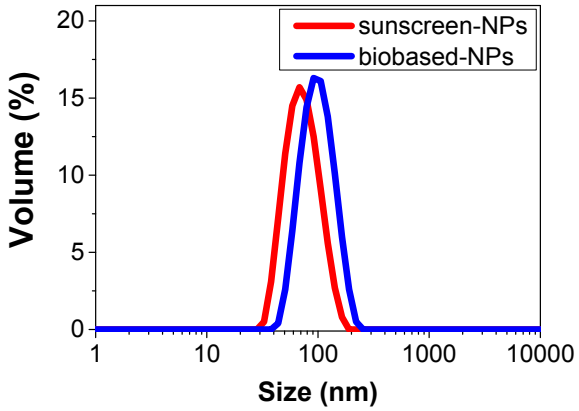

Figure S1. Size distributions as determined by DLS showing the sunscreen-NPs with an average size of 70 nm and the biobased-NPs with an average size of 90 nm.

The SEM imaging shows that both sets of NPs are spherical with sizes consistent with the DLS measurements (Figure S2).

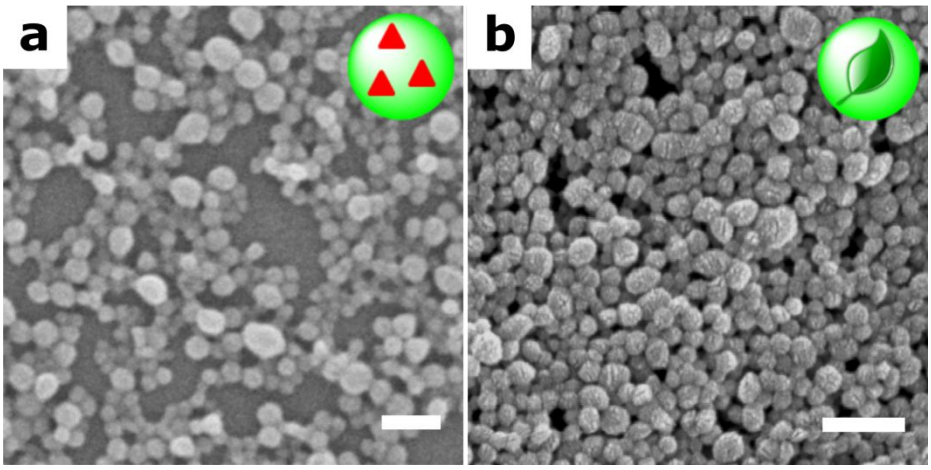

Figure S2. SEM images of (a) sunscreen-NPs and (b) biobased-NPs. Scale bars 200 nm.

The absorbance measurements show that both the sunscreen-NPs and the biobased-NPs demonstrate absorbance over the entire UV spectrum, and the biobased-NPs also absorb up to 450 nm (Figure S3).

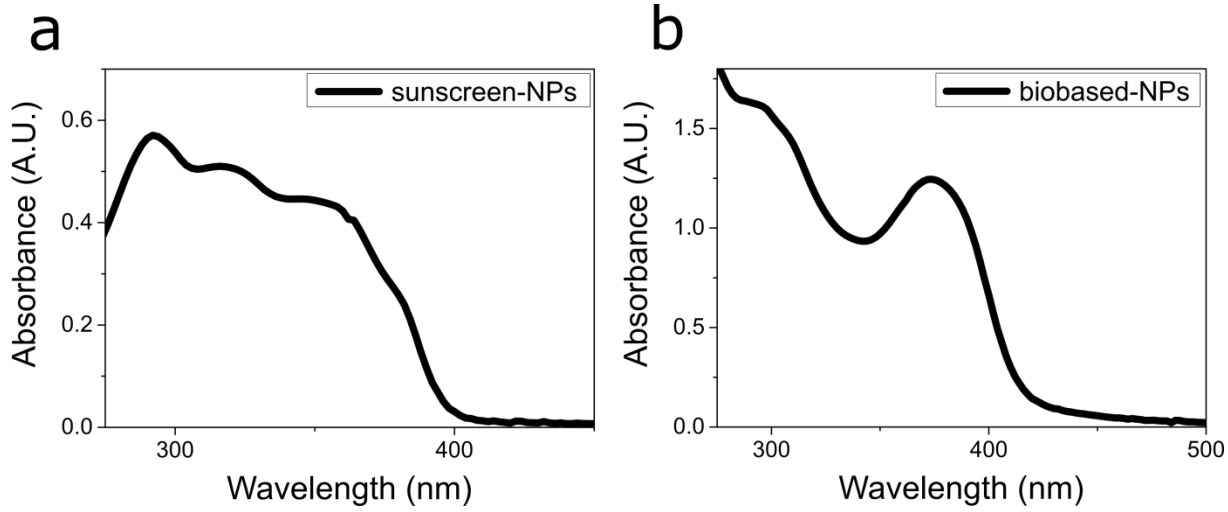

Figure S3. Absorption spectra for (a) sunscreen-NPs and (b) biobased-NPs, both measured at a concentration of 1×10^{-1} g L^{-1}.

The photograph of both NP dispersions in Figure S4 shows that the biobased-NPs are yellow compared to the colourless sunscreen-NPs (slightly blue-tinged due to the Tyndall effect). It is

also worth noting that the fully-biobased particles have been investigated for their environmental durability in wet conditions in previous work, where migration of the UV absorbing molecules are effectively retained within the NPs but some migration can occur.[3] Despite this, EC is insoluble in water and these NPs are known to be stable also at low pH values and across a range of ionic strengths.[4,5]

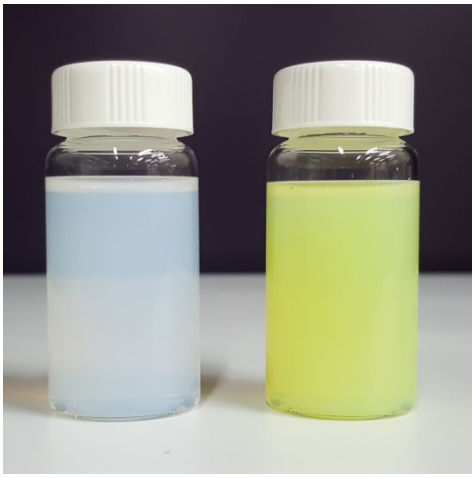

Figure S4. Photo showing dispersions of sunscreen-NPs (left vial) and biobased-NPs (right vial).

2) Nanofibril characterization

The size distributions for the cellulose nanofibrils from a bacterial source and the cellulose nanofibrils from a citrus source are shown in Figure S5. The cellulose nanofibrils from the bacterial and citrus sources have mean average widths of 43 nm and 7 nm respectively.

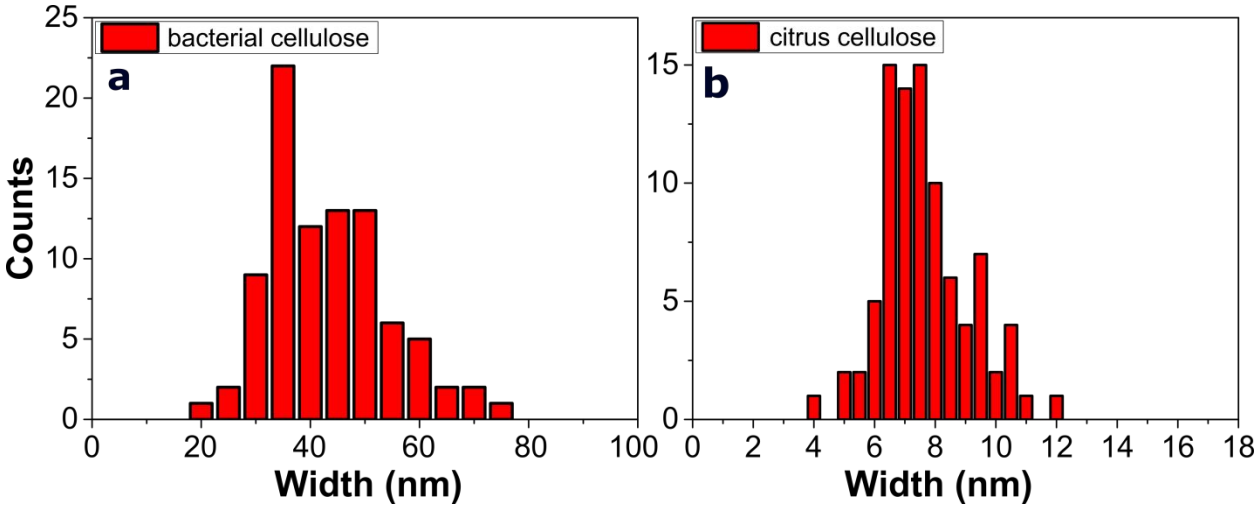

Figure S5. Discrete size distributions for the average width of the cellulose nanofibrils from (a) the bacterial source and (b) the citrus fruits source. Information was obtained from the TEM and SEM images in Figure 1.

3) (Citrus) Films Characterization

When too few sunscreen-NPs or biobased-NPs are used to prepare the films, the films do not completely block UV radiation (Figure S6).

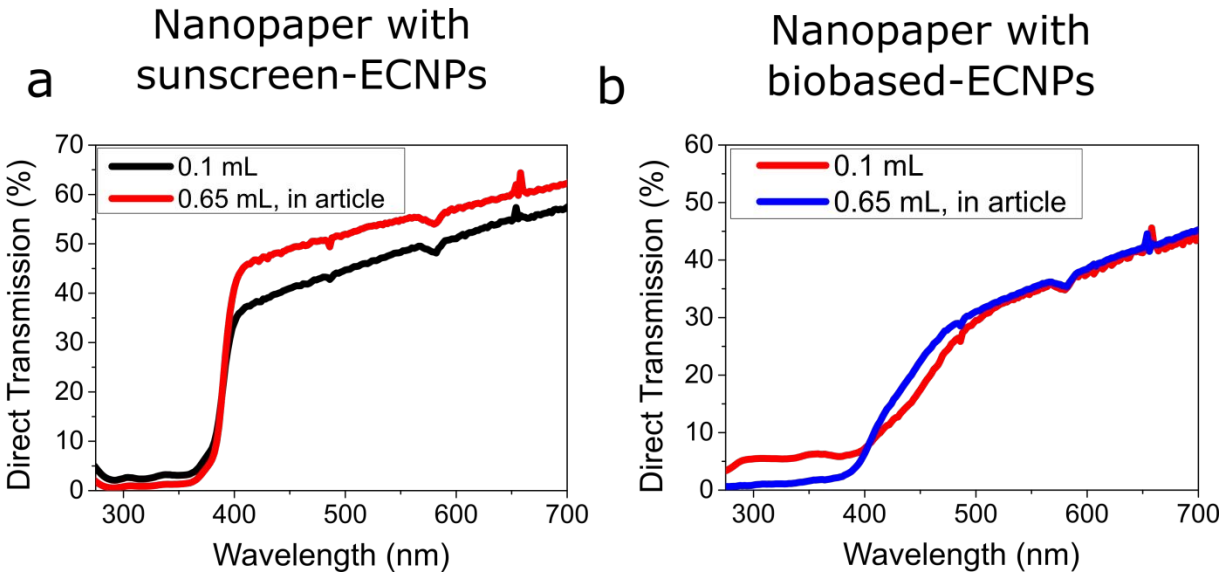

Figure S6. Transmission measurements for the nanopaper films prepared with (a) sunscreen-NPs, and (b) biobased-NPs, showing that when too few NPs are used there is transmission of UV radiation. Concentration of particles used for nanopaper is always 10 g L^{-1} for both the sunscreen-NPs and biobased-NPs.

The film thicknesses for the nanopaper films functionalized with the sunscreen-NPs and the biobased-NPs (shown in Figure 2 in the main article) were 9.6 ± 0.3 µm and 9.5 ± 0.4 µm respectively, determined by measuring the thickness at ten points across the SEM images of the cross sections of both films in Figure S7a-b. Additionally, from SEM imaging of the cross section of another area of the nanopaper film with embedded sunscreen-NPs we found that the NPs are not just distributed on the surface of the films as seen in Figure 2, but also between the layers (Figure S7c).

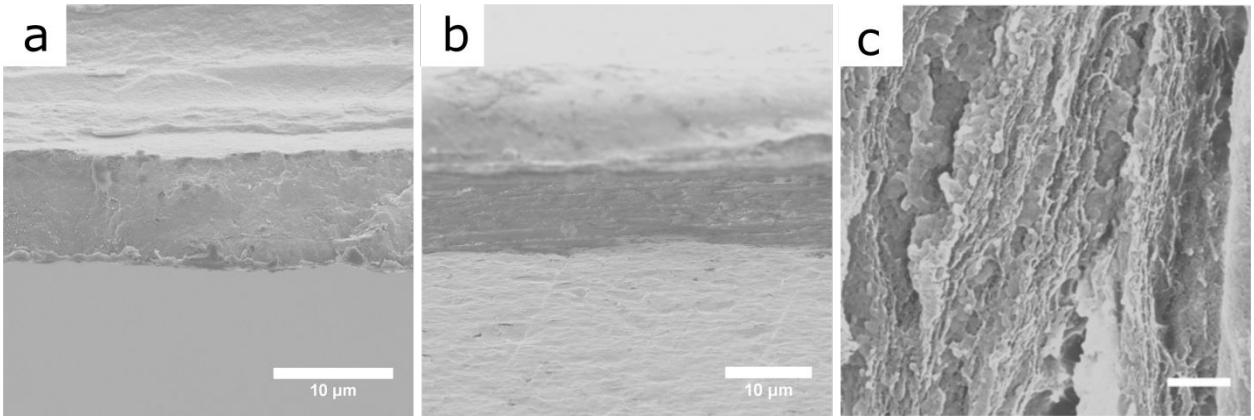

Figure S7. (a-b) SEM images of the cross sections of the functionalized nanopaper films from Figure 2 in the main article, in which (a) is an image of the nanopaper film functionalized with sunscreen-NPs and (b) is an image of the nanopaper film functionalized with biobased-NPs. Both scale bars 10 µm. (c) SEM image of the cross section of a nanopaper film functionalized with sunscreen-NPs from Figure S2 showing that sunscreen-NPs are visible between the layers. Scale bar 500 nm.

The surface roughness values of the prepared films were determined by Atomic Force Microscopy (AFM) from height profiles over a 25 μm^2 area, shown in Figure S8. The surface roughness values are presented as rootmean-square (rms) values. The root mean square (rms) roughness values were measured as 42 nm, 26 nm, 67 nm, and 68 nm for: i) pure bacterial cellulose nanopaper (from Figure 1b) ii) pure citrus cellulose nanopaper (from Figure 1d), iii) citrus cellulose nanopaper functionalized with sunscreen-NPs (from Figure 2a), and iv) citrus cellulose nanopaper functionalized with biobased-NPs respectively (from Figure 2b). These values are all typical for nanopaper[6] which is much smaller than typical values for regular paper (rms values ~5-6 microns[7]).

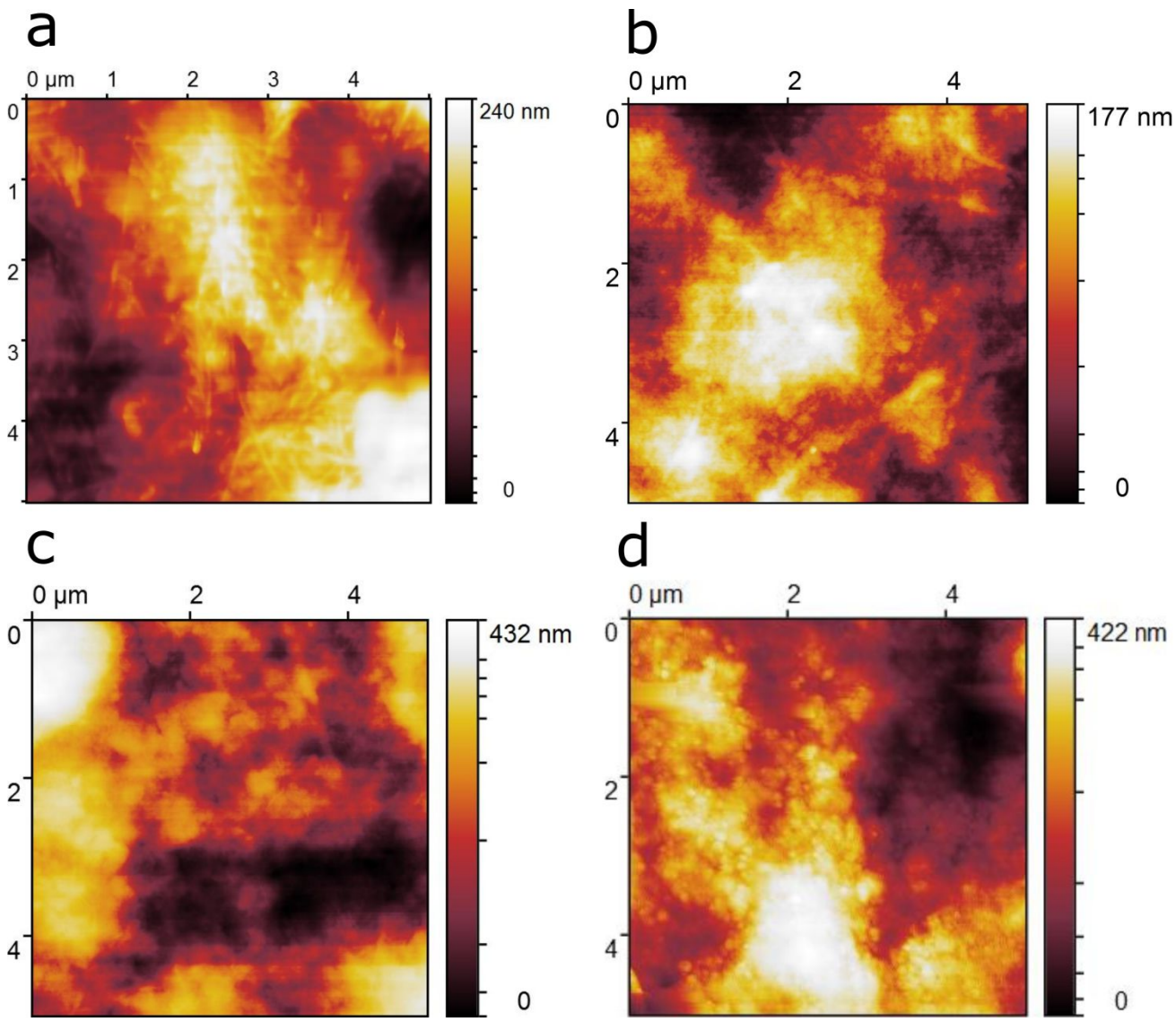

Figure S8. AFM height profiles for: (a) pure bacterial cellulose nanopaper (b) pure citrus cellulose nanopaper, (c) citrus cellulose nanopaper functionalized with sunscreen-NPs, and (d) citrus cellulose nanopaper functionalized with biobased-NPs.

The thermal stability of the nanopaper films was investigated using Thermal Gravimetric Analysis (TGA). We found that the nanopaper films were stable until 180-220^{o}C, where they decomposed significantly up to 450^{o}C (Figure S9). This decomposition can be attributed to the decomposition of cellulose which has been previously observed in the TGA of nanopaper[8].

Interestingly, we find second degradation peaks at ~400°C for two of the films, which we cannot explain. Although interesting, the films have already heavily degraded by this temperature, therefore we emphasize that the important information from this data is that all the films are stable until 180-220°C.

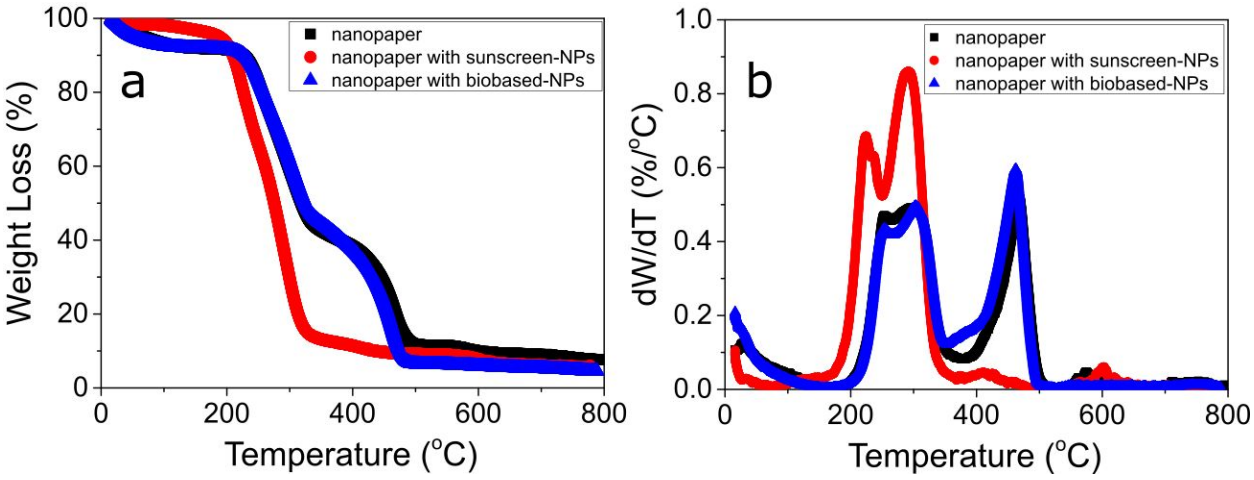

Figure S9. TGA profiles for the pure nanopaper (from Figure 1d), nanopaper with sunscreen-NPs (from Figure 2a), and nanopaper with biobased-NPs (from Figure 2b), indicating their thermal stability under an air atmosphere. (a) Weight loss as a function of temperature. (b) Temperature first derivative weight loss profiles (dW/dT) of the samples.

4) UV-Blocking Nanopaper from Bacterial Cellulose

We found that nanopaper from bacterial cellulose could also be prepared and functionalized in the same way as with citrus cellulose (Figure S10). Fewer NPs were required in order to achieve full UV blockage here – 0.1 mL sunscreen-NPs at 10 g L^{-1} – because the transparency was much lower anyway).

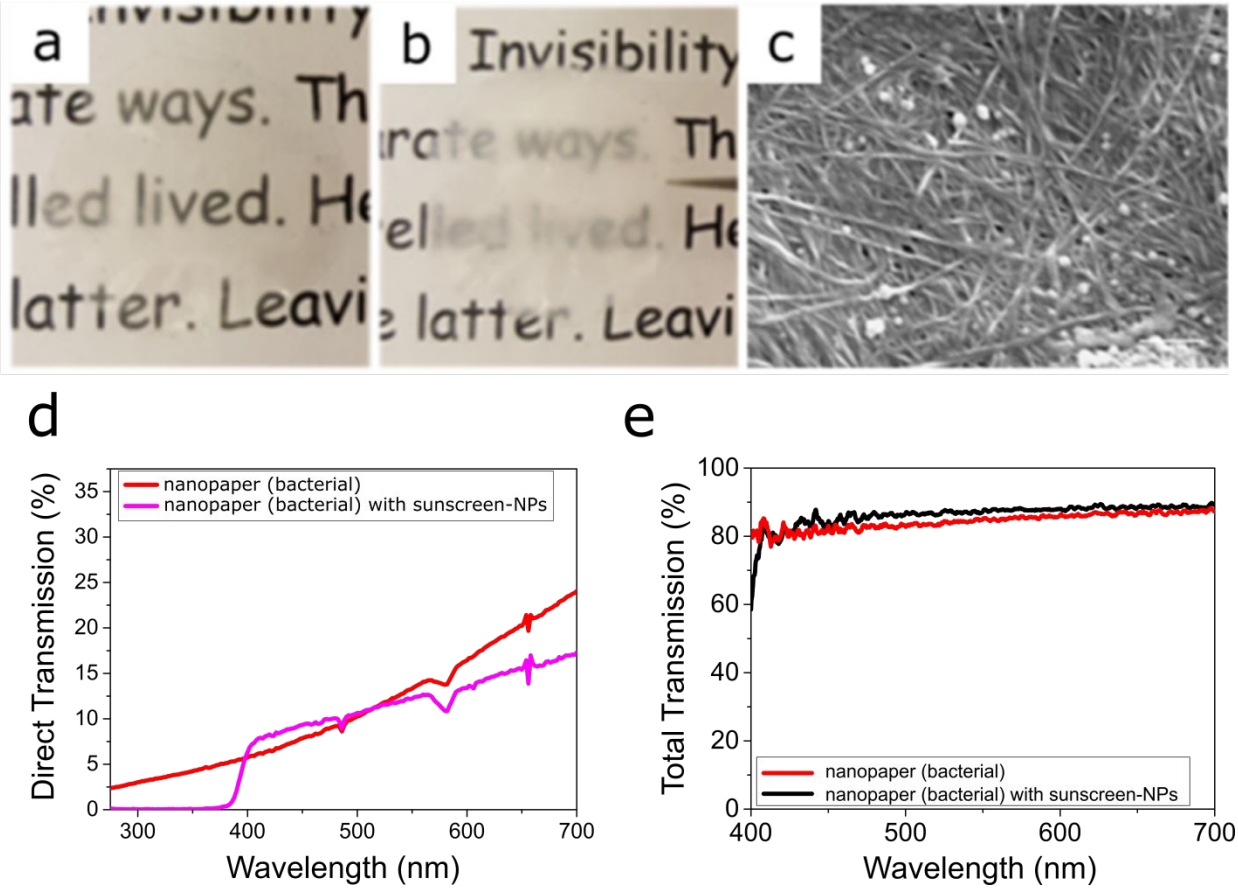

Figure S10. (a-b) Photographs of a nanopaper film using cellulose nanofibrils from a bacterial source (1 mL at 5 g L^{-1}) functionalized with sunscreen-NPs (0.1 mL at 10 g L^{-1}). (c) SEM image of the surface of the nanopaper film clearly showing the large nanofibrils and the particles embedded. Scale bar 500 nm. (d) Direct and (e) total transmission measurements of both the pure bacterial cellulose nanopaper film (the film shown in Figure 1b) and the bacterial cellulose nanopaper film functionalized with the sunscreen-NPs.

References

(1) Saito, T.; Hirota, M.; Tamura, N.; Kimura, S.; Fukuzumi, H.; Heux, L.; Isogai, A. Individualization of Nano-Sized Plant Cellulose Fibrils by Direct Surface Carboxylation Using TEMPO Catalyst under Neutral Conditions. *Biomacromolecules* **2009**, *10*, 1992–1996.

(2) Hayden, D. R.; Imhof, A.; Velikov, K. P. Biobased Nanoparticles for Broadband UV Protection with Photostabilized UV Filters. *ACS Appl. Mater. Interfaces* **2016**, *8*, 32655-32660.

(3) Hayden, D. R.; Kibbelaar, H. V. M.; Imhof, A.; Velikov, K. P. Fully-Biobased UV-Absorbing Nanoparticles from Ethyl Cellulose and Zein for Environmentally Friendly Photoprotection. *RSC Adv.* **2018**, *8*, 25104–25111.

(4) Bizmark, N.; Ioannidis, M. a. Effects of Ionic Strength on the Colloidal Stability and Interfacial Assembly of Hydrophobic Ethyl Cellulose Nanoparticles. *Langmuir* **2015**, *31*, 9282–9289.

(5) Jin, H.; Zhou, W.; Cao, J.; Stoyanov, S. D.; Blijdenstein, T. B. J.; de Groot, P. W. N.; Arnaudov, L. N.; Pelan, E. G. Super Stable Foams Stabilized by Colloidal Ethyl Cellulose Particles. *Soft Matter* **2012**, *8*, 2194.

(6) Sehaqui, H.; Liu, A.; Zhou, Q.; Berglund, L. A. Fast Preparation Procedure for Large, Flat Cellulose and Cellulose/Inorganic Nanopaper Structures. *Biomacromolecules* **2010**, *11*, 2195–2198.

(7) Hsieh, M. C.; Kim, C.; Nogi, M.; Suganuma, K. Electrically Conductive Lines on

Cellulose Nanopaper for Flexible Electrical Devices. *Nanoscale* **2013**, *5*, 9289–9295.

(8) Guo, J.; Uddin, K. M. A.; Mihhels, K.; Fang, W.; Laaksonen, P.; Zhu, J. Y.; Rojas, O. J. Contribution of Residual Proteins to the Thermomechanical Performance of Cellulosic Nanofibrils Isolated from Green Macroalgae. *ACS Sustain. Chem. Eng.* **2017**, *5*, 6978–6985.